NASA Technical Memorandum 106263
AIAA–93–3105
ICOMP–93–24; CMOTT–93–10

A Galilean and Tensorial Invariant k–ε Model for Near Wall Turbulence

Z. Yang and T.H. Shih
Institute for Computational Mechanics in Propulsion and
Center for Modeling of Turbulence and Transition
Lewis Research Center
Cleveland, Ohio

Prepared for the
24th Fluid Dynamics Conference
sponsored by the American Institute of Aeronautics and Astronautics
Orlando, Florida, July 6–9, 1993

NASA

INSTITUTE FOR COMPUTATIONAL MECHANICS IN PROPULSION
NASA ICOMP Lewis Research Center Ohio Aerospace Institute

A GALILEAN AND TENSORIAL INVARIANT κ-ε MODEL FOR NEAR WALL TURBULENCE

Z. Yang* and T.H. Shih†
Institute for Computational Mechanics in Propulsion
Lewis Research Center
Cleveland, Ohio 44135
and Center for Modeling of Turbulence and Transition
National Aeronautics and Space Administration
Lewis Research Center
Cleveland, Ohio 44135

Abstract

A $k-\epsilon$ model is proposed for wall bounded turbulent flows. In this model, the eddy viscosity is characterized by a turbulent velocity scale and a turbulent time scale. The time scale is bounded from below by the Kolmogorov time scale. The dissipation rate equation is reformulated using this time scale and no singularity exists at the wall. A new parameter $R = \frac{k}{S\nu}$ is introduced to characterize the damping function in the eddy viscosity. This parameter is determined by local properties of both the mean and the turbulent flow fields and is free from any geometry parameter. The proposed model is then Galilean and tensorial invariant. The model constants used are the same as in the high Reynolds number Standard k-ϵ Model. Thus, the proposed model will be also suitable for flows far from the wall. Turbulent channel flows and turbulent boundary layer flows with and without pressure gradients are calculated. Comparisons with the data from direct numerical simulations and experiments show that the model predictions are excellent for turbulent channel flows and turbulent boundary layers with favorable pressure gradients, good for turbulent boundary layers with zero pressure gradients, and fair for turbulent boundary layer with adverse pressure gradients.

1. Introduction

In turbulence modeling, the k-ϵ model is the most widely used model in engineering calculations. The Standard $k-\epsilon$ Model[1,2] was devised for high Reynolds number turbulent flows and is traditionally used in conjunction with wall functions when it is applied to wall bounded turbulent flows. However universal wall functions do not exist in complex flows and it is thus necessary to develop a form of $k-\epsilon$ model equations which can be integrated down to the wall.

Jones and Launder[3] were the first to propose a low Reynolds number $k-\epsilon$ model for near wall turbulence, which was then followed by a number of similar $k-\epsilon$ models. A critical evaluation of the pre-1985 models was made by Patel et al.[4]. More recently proposed models are found in Shih[5] and Lang and Shih[6]. Three major deficiencies can be pointed out about existing $k-\epsilon$ models. (Some of the models may have only one or two of the three deficiencies.) First, a near wall pseudo-dissipation rate was introduced to remove the singularity in the dissipation rate equation at the wall. The definition of the near wall pseudo-dissipation rate was quite arbitrary. Second, the model constants were different from those of the Standard $k-\epsilon$ Model, making the near wall models less capable of handling flows containing both high Reynolds number turbulence and near wall turbulence, which is often the case for a real flow situation. Patel et al.[4] put as the first criterion the ability of the near wall models to be able to predict turbulent free shear flows. Third, the variable y^+ is used in the damping function f_μ of the eddy viscosity formulae. Since the definition of y^+ involves u_τ, the friction velocity, any model containing y^+ can not be used in flows with separation. In addition, y^+ may not be well defined for flows with complex geometry.

In an earlier paper by the authors[7] (referred as YS here after), a time scale based $k-\epsilon$ model for near wall turbulence was proposed. In this model, $k^{1/2}$ was chosen as the turbulent velocity scale. The time scale was bounded from below by the Kolmogorov time scale. When this time scale is used to reformulate the dissipation rate equation, there is no singularity at the wall and the introduction of a pseudo-dissipation rate is avoided. The model constants were exactly the same as those in the Standard $k-\epsilon$ Model, which ensures the correct performance of the model far from the wall. The damping function in YS was proposed as a function of $R_y = \frac{k^{1/2}y}{\nu}$ instead of y^+ Thus, the model can be used for flows with separation and reattachment.

However, the R_y dependence in the damping function makes the model coordinate dependent. It also creates some ambiguity when the model is used for complex geometries, for example, a corner flow. Similar problem also exists in most existing $k-\epsilon$ models.

*Research Scientist
†Technical Leader

The aim of the present paper is to remove this deficiency while keeping the good performance of YS. This is achieved by introducing a new parameter R, to be defined and discussed in section 2, as the independent variable of the damping function in the eddy viscosity. The introduction of R also makes the proposed model Galilean and tensorial invariant. The proposed model is then calculated for turbulent channel flows at different Reynolds numbers and for turbulent boundary layer flows at zero pressure gradient, favorable pressure gradient, and adverse pressure gradient. The numerical aspects of the computation are briefly discussed in section 3. The results of the model calculations and the comparisons with the data from experiments and direct numerical simulations are shown in section 4. Section 5 concludes the paper.

2. Near wall $k-\epsilon$ model

In turbulence modeling, the instantaneous quantities of an incompressible flow are decomposed into the mean and the fluctuating parts, i.e., $\tilde{u}_i = U_i + u_i$, $\tilde{p} = P + p$. The mean field U_i satisfies the following continuity equation and Reynolds averaged Navier-Stokes equation:

$$U_{i,i} = 0 \tag{1}$$

$$\dot{U}_i + U_j U_{i,j} = -\frac{1}{\rho} P_i + \nu U_{i,jj} - \overline{u_i u_j}_{,j} \tag{2}$$

where the Reynolds stress term, $-\overline{u_i u_j}$, must be modeled.

In an eddy viscosity model, one assumes that the Reynolds stress is related to the mean field by

$$-\overline{u_i u_j} = \nu_T (U_{i,j} + U_{j,i}) - \frac{2}{3} k \delta_{ij}, \tag{3}$$

where ν_T is the eddy viscosity and k is the turbulent kinetic energy.

In the near wall $k-\epsilon$ model proposed by YS, the eddy viscosity is written as

$$\nu_T = c_\mu f_\mu k T_t \tag{4}$$

where

$$T_t = \frac{k}{\epsilon} + (\frac{\nu}{\epsilon})^{1/2} \tag{5}$$

is the time scale for turbulent flows. The first term on the right hand side of the above equation is the conventionally used expression for the turbulent time scale. The second term is the Kolmogorov time scale. As the wall is approached, the conventionally used expression for turbulent time scale, k/ϵ, approaches to zero due to the boundary condition for k. However, as it was shown in YS based on a local Taylor series expansion of the instantaneous velocity field, the turbulent time scale should approach to the Kolmogorov time scale near the wall rather than zero. The turbulent time scale given by equation (5) has the properties that the turbulent time scale is given by the Kolmogorov time scale near the wall and the turbulent time scale is given by the conventionally used expression (k/ϵ) far away from the wall, where Kolmogorov time scale is much smaller than k/ϵ.

k and ϵ are found from solutions of the following modeled transport equations

$$\frac{Dk}{Dt} = [(\nu + \frac{\nu_T}{\sigma_k}) k_{,j}]_{,j} - \overline{u_i u_j} U_{i,j} - \epsilon \tag{6}$$

$$\frac{D\epsilon}{Dt} = [(\nu + \frac{\nu_T}{\sigma_\epsilon}) \epsilon_{,j}]_{,j} + \frac{(-C_{1\epsilon} \overline{u_i u_j} U_{i,j} - C_{2\epsilon} \epsilon)}{T_t} + C_\epsilon \nu \nu_T U_{i,jk} U_{i,jk}. \tag{7}$$

The turbulent time scale given by equation (5) is used to reformulate the dissipation rate equation (7). Since the turbulent time scale is always positive, the dissipation rate equation does not have any singularity as the wall is approached. The argument on the time scale for near wall turbulence and the use of the Kolmogorov time scale for near wall turbulence modeling are also discussed by other researchers, see Durbin[8], for example.

f_μ in equation (4) is the damping function which is introduced to account for the effect of the wall on the eddy viscosity. In YS, f_μ was given as a function of $R_y = k^{1/2} y/\nu$. The parameter R_y has the advantage over the commonly used $y^+ = u_\tau y/\nu$ in that it could be used for flows with separation and reattachment. However, the appearance of y in the damping function makes the model non-tensorial invariant. In addition, in complicated geometry situations such as corner flows, the meaning of y is ambiguous.

To overcome this deficiency, we introduce a new parameter R, which is defined as

$$R = \frac{k}{S\nu} \tag{8}$$

where S is the modulus of the strain rate tensor S_{ij} of the mean velocity field and is given by

$$S = (2 S_{ij} S_{ij})^{1/2}. \tag{9}$$

The parameter R defined above is expressed in terms of the local variables of the field and is thus

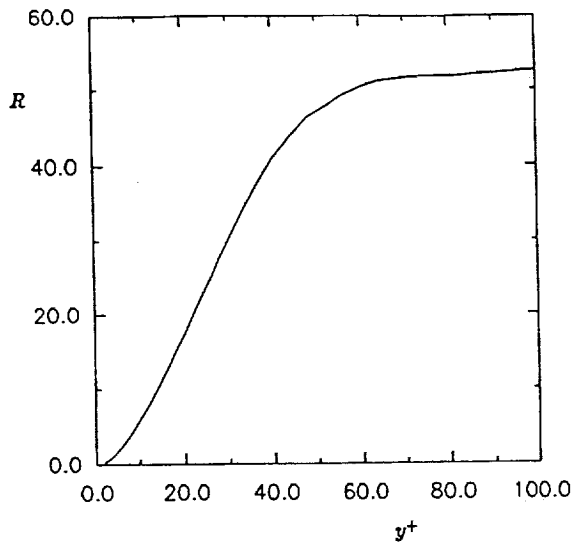

Figure 1: Variation of R for turbulent channel flow at $Re_\tau = 180$.

coordinate independent. The physical meaning of R can be explained as follows,

$$R = \frac{k}{S\nu} = \frac{k^2}{\epsilon\nu} / \frac{Sk}{\epsilon}; \qquad (10)$$

R is then the ratio of two important physical parameters: the turbulent Reynolds number and the time scale ratio of the turbulence to the mean flow. The variation of R with the wall distance y^+ for the case of turbulent channel flow at $Re_\tau = 180$ is shown in figure 1. The gradual and monotonic increase of R with y^+ in the near wall region makes R an ideal candidate for constructing the damping function.

In the present study, the form of the damping function is chosen as

$$f_\mu = [1 - exp(-a_1 R - a_2 R^2 - a_3 R^3)]^{1/2} \qquad (11)$$

where $a_1 = 3\text{x}10^{-4}$, $a_3 = 6\text{x}10^{-5}$, $a_5 = 2\text{x}10^{-6}$. These constants are obtained by calibrating the model predictions for the turbulent channel flow at $Re_\tau = 180$ against the direct numerical simulation date of Kim et al.[9]

Near the wall, the shear stress $-\overline{uv}$ should behave as $O(y^3)$, according to the local Taylor series analysis. Since k is $O(y^2)$ and the time scale T_t is finite, we would require the damping function to have a near wall behavior of $O(y)$. From equation (8) and equation (11), it is seen that as $y \to 0$, $R \to 0$ as $O(y^2)$, which gives $f_\mu \to 0$ as $O(y)$. Thus, the near wall asymptotic behavior for the shear stress is satisfied. Far from the wall, R is large and $f_\mu \to 1$.

The other effect in the modeling of the near wall turbulence is the effect of the inhomogeneity of the mean field which introduces a secondary source term in the dissipation rate equation. This is represented by the last term on the right hand side of equation (7). A term of this form in the dissipation rate equation was suggested by Jones and Launder[3], and Shih[5]. The effect of this term is confined to the near wall region and is most prominent in the buffer layer. Away from the wall, this term becomes much smaller than the other terms in the dissipation rate equation.

Equations (4), (6), and (7) along with the eddy viscosity given by equation (11) are the $k-\epsilon$ equations proposed in the present paper. The model could be used for complex flows, flows with separation and reattachment, for example. Since all the quantities are expressed in the local variables, the model can be incorporated in a general purpose CFD code, particularly a code with unstructured grid.

The model constants, c_μ, $C_{1\epsilon}$, $C_{2\epsilon}$, σ_k, σ_ϵ, are chosen to be the same as those in the Stanford $k-\epsilon$ Model, i.e. $c_\mu = 0.09$, $C_{1\epsilon} = 1.44$, $C_{2\epsilon} = 1.92$, $\sigma_k = 1.0$, $\sigma_\epsilon = 1.3$. The value of C_ϵ is chosen to be equal to 1.0 based on the model performance for turbulent channel flows. Away from the wall, the present model reduces to the Standard $k-\epsilon$ Model. Thus, it is only necessary to assess the performance of the model for wall bounded flows.

The boundary condition for ϵ on the wall is determined by applying equation (6) at the wall, which gives

$$\epsilon_w = \nu k_{,yy}.$$

In this study, the following boundary condition for ϵ, which is mathematically equivalent to the above but computationally much more robust, is used.

$$\epsilon_w = 2\nu(\frac{dk^{1/2}}{dy})^2 \qquad (12)$$

3. Numerical aspects

Boundary layer approximation is used in the calculations shown below. An implicit finite difference scheme is used to solve the momentum equation and the transport equations for k and ϵ. The coefficients for the convective terms are lagged one step in the marching direction and the source terms in the k and ϵ equations are linearized in such a way that numerical stability is ensured.

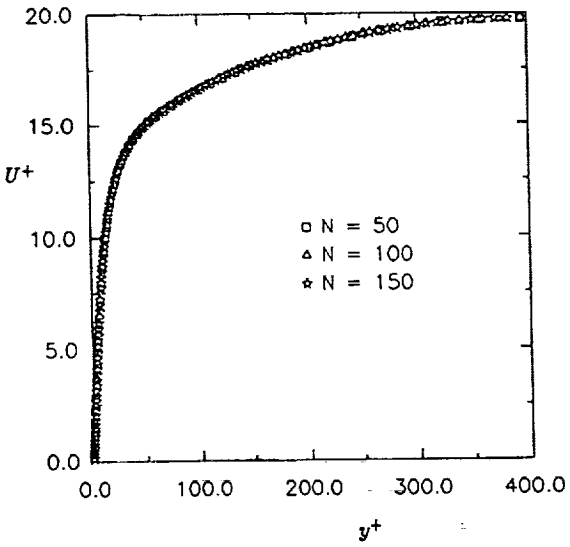

Figure 2: Computation of turbulent channel flow at $Re_\tau = 395$ with different number of grid points.

A variable grid spacing is used to resolve the sharp gradient near the wall. The grid distribution is controlled by $\delta y_i/\delta y_{i-1} = \alpha$. Both α and the total number of the grid, N, are varied to ensure the grid independence of the numerical results. The marching step size, δx, is also varied to ensure accuracy. In the calculations shown in the next section, these parameters are changed such that the solution has a less than 1.0% error. Typically, the grids used are specified by $N = 150$ and $\alpha = 1.05$. It is also found that the solution is not sensitive to the number of the grid points as long as there are two points in $y^+ < 1$. Figure 2 shows calculations for the turbulent channel flow at $Re_\tau = 395$ with N varying from 50 to 150 and α changes accordingly such that α^N remains basically the same. It is seen that the results for different N are almost identical.

4. Results and discussions

Turbulent channel flows at different Reynolds numbers and turbulent boundary layers with zero pressure gradient, favorable pressure gradient, and adverse pressure gradient are calculated using the present model. The following shows the computational results along with the available experimental data and data from direct numerical simulations. For some cases, the predictions of the Jones-Launder model and the Chien's model[10] are also shown. These two models are chosen because the Jones-Launder model is the first $k-\epsilon$ model for near wall turbulence while the Chien's model is known to perform quite well for turbulent boundary layer flows.

Two dimensional fully developed channel flows were calculated first. These flows are attractive for model testing because they have self-similar solutions so that the initial conditions do not have to be accurately specified. These flows are very simple and solutions can be found very efficiently; yet, the effects of the wall on turbulent shear flow are still present. In addition, DNS data providing detailed flow information are available for comparisons. Computations are carried out for 2D fully developed turbulent channel flows at $Re_\tau = 180$ and $Re_\tau = 395$, respectively. Figures 3-6 show the profiles of the mean velocity, shear stress, turbulent kinetic energy , and the dissipation rate, respectively, for the case of $Re_\tau = 180$. Both the dependent variable and the independent variables are represented in wall units by normalization through u_τ and ν. The predictions of the Jones-Launder model and the Chien's model are also shown. These predictions are compared with the DNS data. It is found that the present model gives the right location of the maximum value of the dissipation rate. The center line velocity, which corresponds to the skin friction coefficient, is also well predicted. The corresponding results for the case of $Re_\tau = 395$ are shown in figures 7-10.

Like the 2D fully developed channel flows, zero pressure gradient (ZPG) turbulent boundary layer flows over a flat plate also give a self-similar solution. Thus, arbitrary profiles could be used as the initial conditions and the solution would develop into its similarity form. In our case, constant values are assigned to the velocity, turbulent energy and the dissipation rate. The exact values for the initial profiles are immaterial as long as the turbulent boundary gets generated. The boundary conditions used are that, at the free stream, the velocity reaches that of the freestream and the gradients for the turbulent energy and the dissipation rate are set to zero. Figures 11-14 show the predicted velocity profile, shear stress, turbulent energy, and dissipation rate at $Re_\theta = 1410$. The DNS data of Spalart[11] is also shown. Again, the predictions from the Jones-Launder model and the Chien's model are shown for comparisons.

The computations were also carried out for larger Reynolds number up to $Re_\theta = 16000$. The comparison is made between the model predictions and the experimental results of Wieghardt and Willmann[14] for zero pressure gradient turbulent boundary layers. Figure 15 shows the results of the skin friction coefficient as a function of Re_θ. In figure 16, the velocity

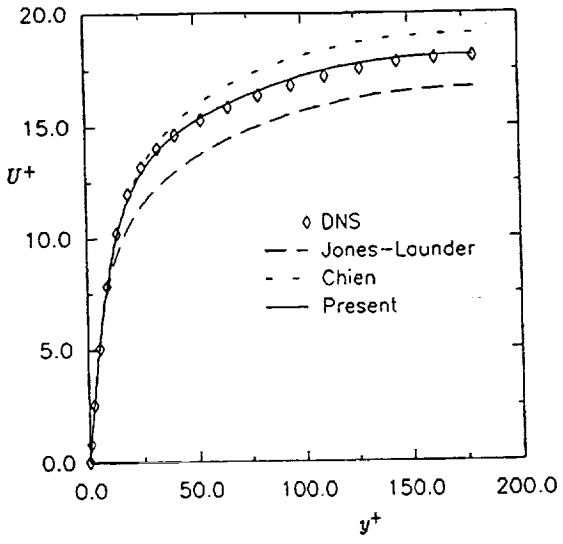

Figure 3: Mean velocity profile for turbulent channel flow at $Re_\tau = 180$.

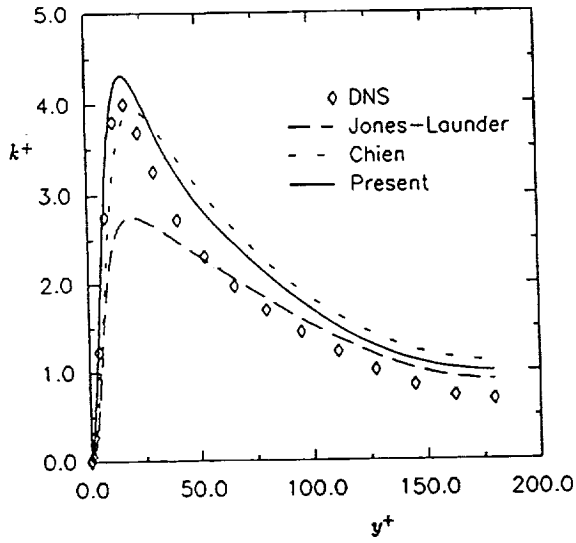

Figure 5: Turbulent kinetic energy for turbulent channel flow at $Re_\tau = 180$.

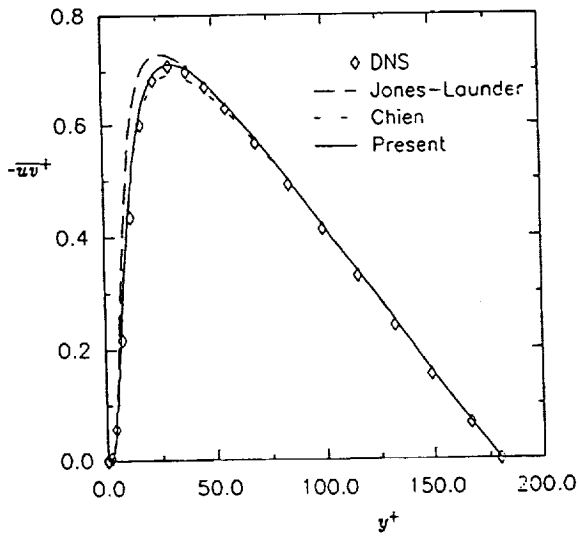

Figure 4: Turbulent shear stress for turbulent channel flow at $Re_\tau = 180$.

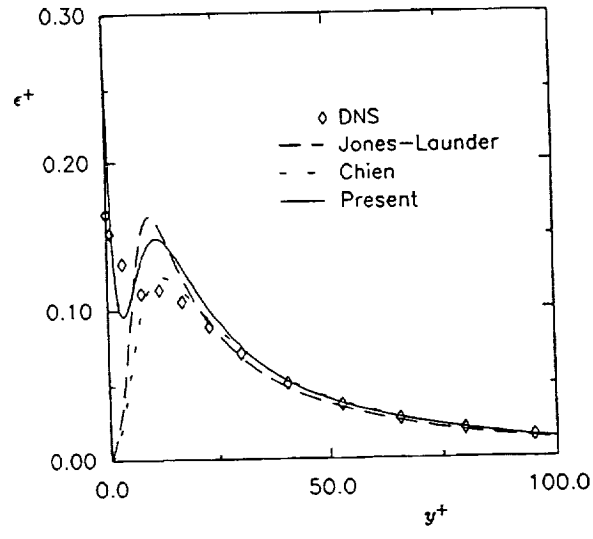

Figure 6: Turbulent dissipation rate for turbulent channel flow at $Re_\tau = 180$.

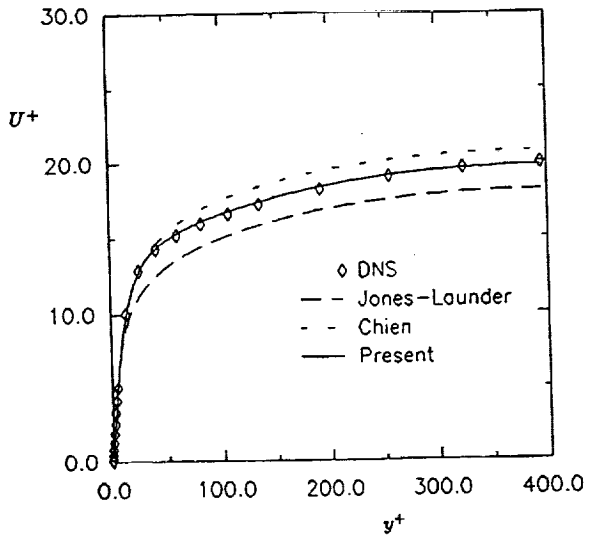

Figure 7: Mean velocity profile for turbulent channel flow at $Re_\tau = 395$.

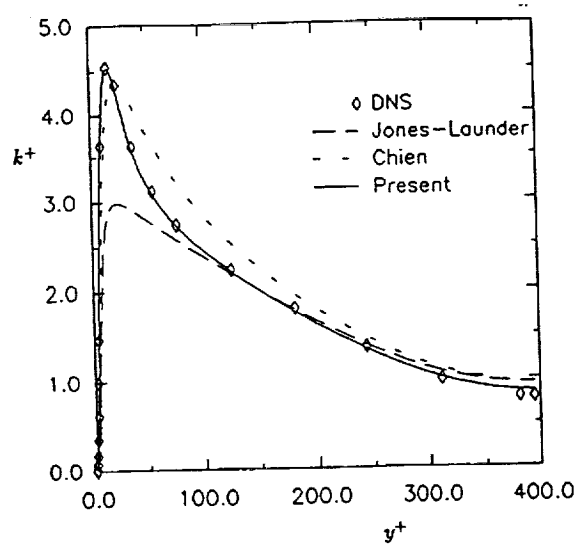

Figure 9: Turbulent kinetic energy for turbulent channel flow at $Re_\tau = 395$.

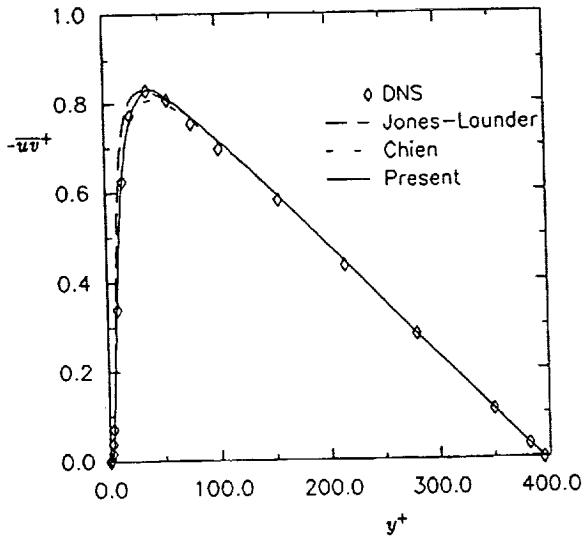

Figure 8: Turbulent shear stress for turbulent channel flow at $Re_\tau = 395$.

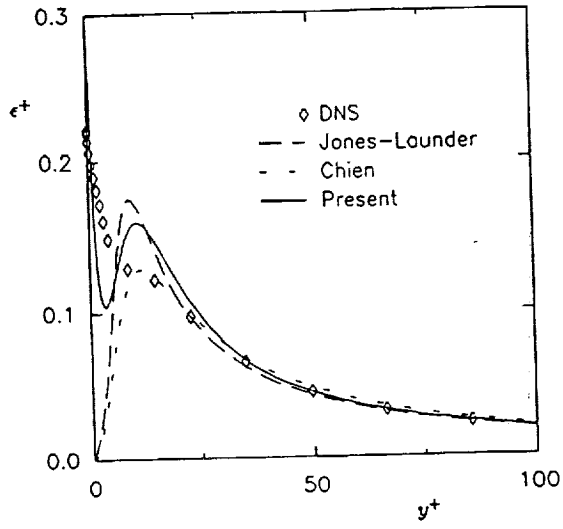

Figure 10: Turbulent dissipation rate for turbulent channel flow at $Re_\tau = 395$.

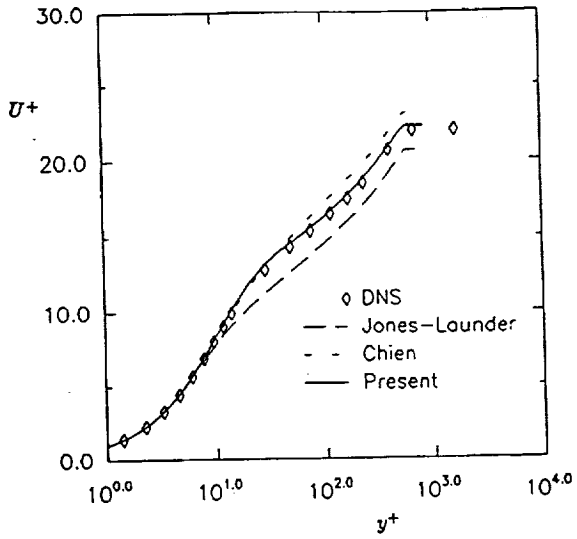

Figure 11: Mean velocity profile for ZPG turbulent boundary layer at $Re_\theta = 1410$.

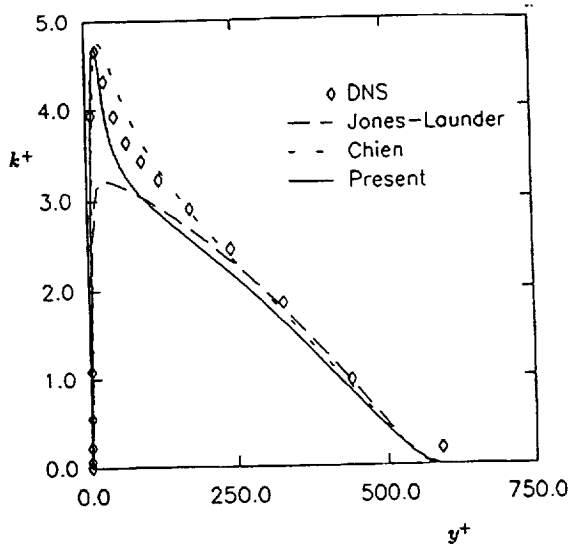

Figure 13: Turbulent kinetic energy for ZPG turbulent boundary layer at $Re_\theta = 1410$.

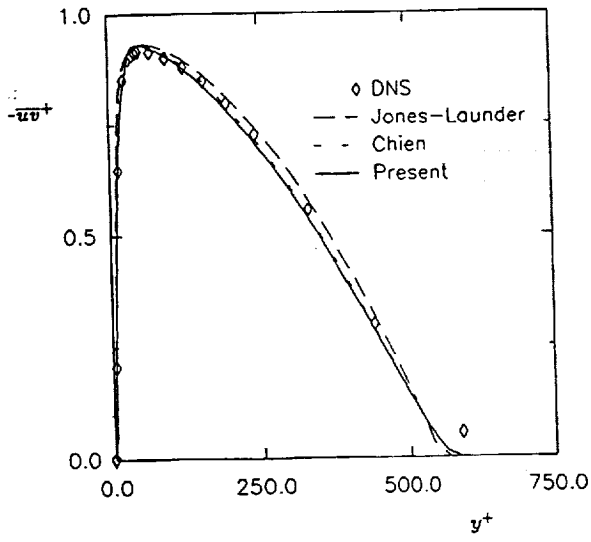

Figure 12: Turbulent shear stress for ZPG turbulent boundary layer at $Re_\theta = 1410$.

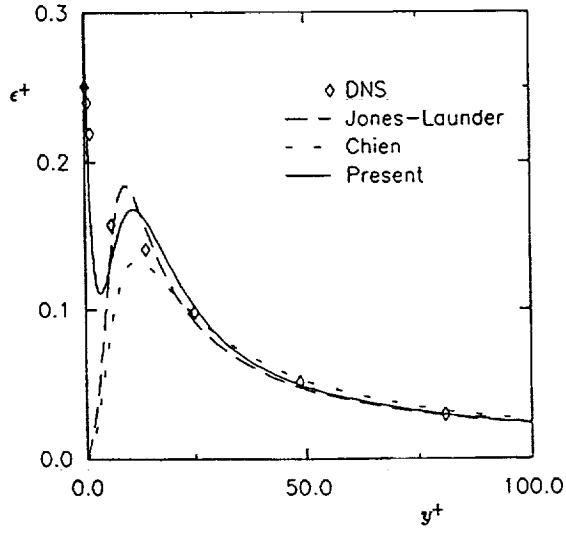

Figure 14: Turbulent dissipation rate for ZPG turbulent boundary layer at $Re_\theta = 1410$.

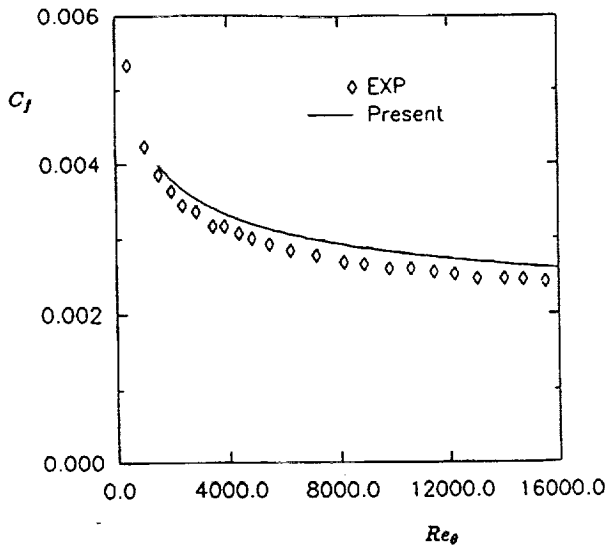

Figure 15: Skin friction for ZPG turbulent boundary layer.

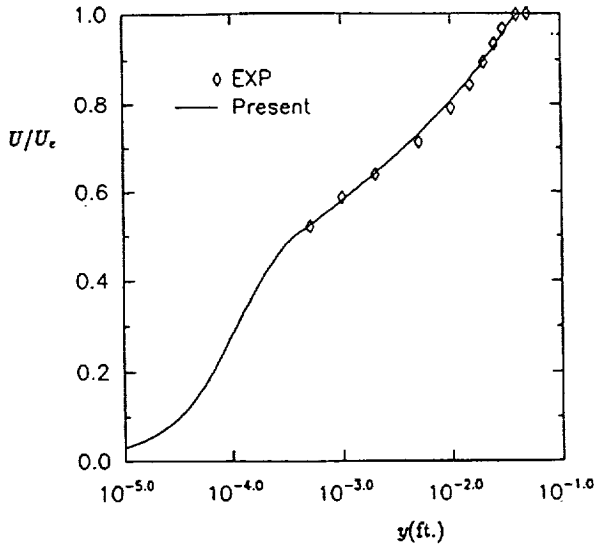

Figure 16: Velocity profile for ZPG turbulent boundary layer at $Re_\theta = 8900$.

profile at $Re_\theta = 8900$ is presented. The predicted value of C_f is a few percent higher than that of the experiment. The predicted velocity profile agrees well with the experiment.

When the turbulent boundary layer is subject to a pressure gradient, the similarity solution ceases to exist. In this case, accurate description of the initial conditions for the velocity profile and the profiles of turbulence quantities (turbulent energy and dissipation rate) are very important. While experiment could provide the velocity profile at the upstream location, information on the turbulence quantities (especially the dissipation rate) is hardly available. In this study, the issue of the initial condition is dealt with in the following manner. We assume that the turbulent boundary layer develops under zero pressure gradient until it passes into the working section of the wind tunnel, where the experimental measurements are made. The connecting point between this virtual flat plate boundary layer and the real boundary layer with the pressure gradient is determined by the value of Re_θ which is found by the experiment.

The boundary conditions are specified in the same way as in the case of a flat plate boundary layer. At the wall, both the velocity and the turbulent energy are equal to zero while the dissipation rate is given by equation (12). At the free stream, zero gradients are assigned to the turbulent energy and its dissipation rate. The mean velocity approaches that of the free stream, which is determined by the experiment and is related to the pressure gradient of the flow.

The turbulent boundary layer studied by Herring and Norbury[13] was chosen as a test case for the turbulent boundary layer with a favorable pressure gradient. At the first point of the working section of the experiment, $Re_\theta = 3400$. Thus, profiles of the mean velocity and turbulent quantities (k and ϵ) of a flat plate boundary layer at $Re_\theta = 3400$ are used to provide the initial conditions. With the initial conditions given, the calculation of the boundary layer is then carried out downstream. The result for the skin friction coefficient is shown in figure 17, and the result for the mean velocity at x = 4ft is shown in figure 18. The distances, x and y, are in physical units while the skin friction and the velocity are normalized by the freestream velocity at the streamwise location under consideration. It is seen that predictions for both the velocity profile and the skin friction are excellent.

The turbulent boundary layer studied by Samuel and Joubert[14] was chosen as a test case for the turbulent boundary layer with an adverse pressure gradient. In this flow, the initial conditions are specified at x = 0.855m, where $Re_\theta = 5470$. First, the predicted skin friction is shown in figure 19 along with

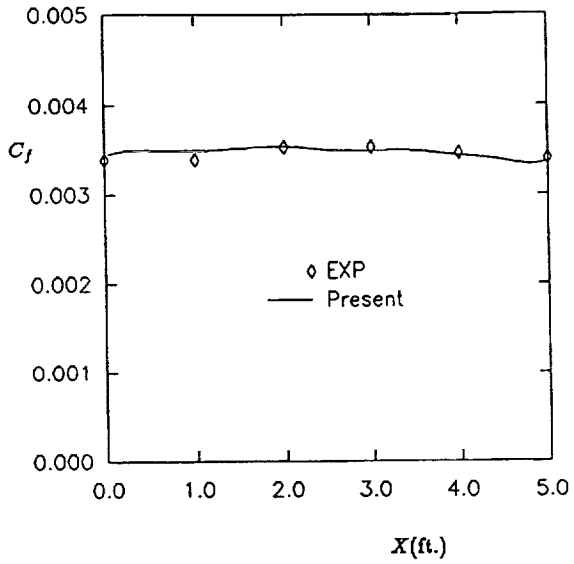

Figure 17: Skin friction for FPG turbulent boundary layer.

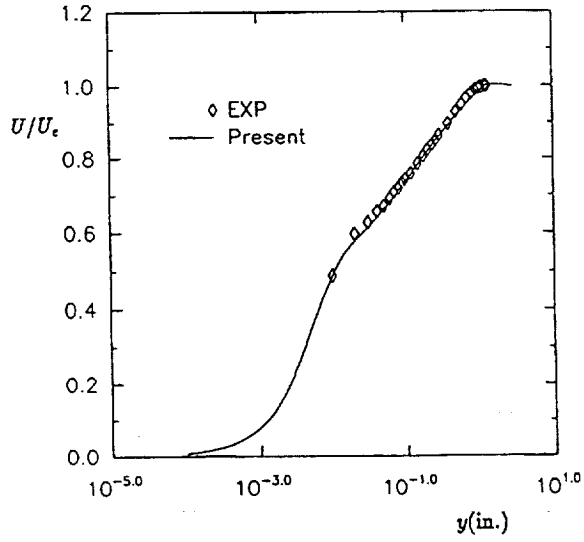

Figure 18: Velocity profile for FPG turbulent boundary layer at $X = 4.0$ft.

the experimental values. The predicted skin friction is higher than that from the experiment, especially in the latter portion of the of the experimental test section where the adverse pressure gradient is fairly strong. The predicted velocity profiles at two different locations ($X = 2.4m$ and $X = 3.04m$, respectively.) are shown in figure 20, along with the experimental data. It is seen that the velocity profiles are in reasonable agreement with the experimental data.

5. Conclusions

By introducing the parameter R, we have successful removed the y dependence of the damping function in YS. Now, the current model is free from the three deficiencies of other existing near wall $k-\epsilon$ models mentioned in the introduction. First, the proposed model uses the same set of model constants as that used in the Standard $k-\epsilon$ Model and away from the wall the proposed model will reduce to the Standard $k-\epsilon$ Model. Thus, the proposed model would be applicable for both near wall turbulence and high Reynolds number turbulence. Second, the proposed model uses a time scale which has the Kolmogorov time scale as its lower bound. By using this time scale to reformulate the dissipation equation, the singularity in the dissipation rate equation of the Standard $k-\epsilon$ Model is removed as the wall is approached and the equation can be integrated to the wall. This renders the introduction of pseudo-dissipation unnecessary. Third, the proposed model uses R as its independent variable in the damping function. This allows the model to be used in more complicated flow situations, flows with separation, for example. In addition, this makes the proposed model Galilean and tensorial invariant. Since all the quantities in the proposed model are given in the local variables, the proposal model is very suitable for general purposed CFD code with unstructured grid.

Turbulent channel flows at different Reynolds numbers and turbulent boundary layers with/without pressure gradient are calculated using the present model. At low Reynolds number, the comparison between the DNS data and the present model is found to be excellent. At higher Reynolds numbers, the velocity profiles are well predicted in all cases. However, the predicted skin friction does not respond adequately with the pressure gradient. All the other existing $k-\epsilon$ models suffer from the same deficiency, as pointed out by Wilcom[15]. Currently, effort is being made to improve the model in this aspect.

It should be mentioned that the model is computationally robust. Arbitrary initial profiles can be used for turbulent channel flows and flat plate boundary layers when similarity solutions exist. The predicted

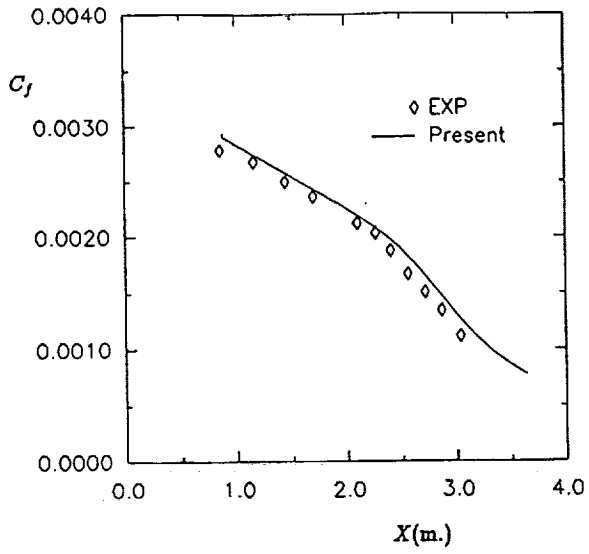

Figure 19: Skin friction for APG turbulent boundary layer.

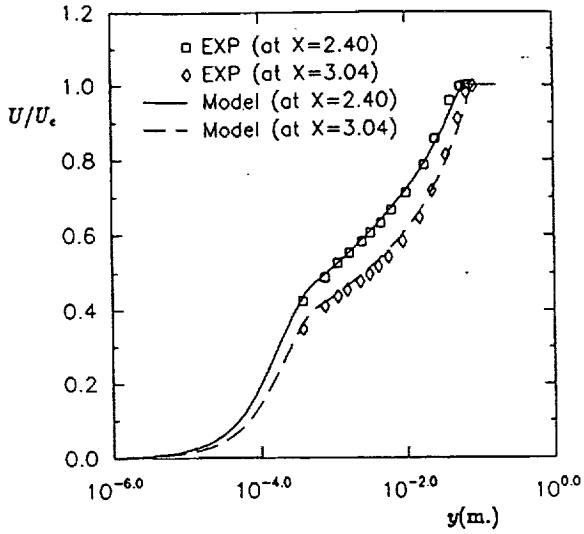

Figure 20: Velocity profiles for APG turbulent boundary layer at $X = 2.4$m and $X = 3.04m$.

solution is also found to be quite insensitive to the number of grid points.

Acknowledgement

The DNS data used was kindly made available to us by Dr. N. Mansour of NASA Ames Research Center.

References

[1]Launder, B.E., and Spalding, D.B., "The Numerical Computation of Turbulent Flow," *Computer Methods in Applied Mechanics and Engineering*, Vol. 3, 1974, pp 269-289.

[2]Rodi, W., *Turbulence Models and Their Application in Hydraulics*, Book Pub. of International Association for Hydraulic Research, Delft, the Netherlands, 1980.

[3]Jones, W.P., and Launder, B.E., "The Calculation of Low-Reynolds Number Phenomena with a Two-Equation Model of Turbulence," *International Journal of Heat and Mass Transfer*, Vol.16, 1973, pp 1119-1130.

[4]Patel, V.C., Rodi, W., and Scheuerer, G., "Turbulence Models for Near-Wall and Low-Reynolds Number Flows: a Review," *AIAA Journal*, Vol. 23, 1985, pp 1308-1319.

[5]Shih, T.H., "An Improved $k-\epsilon$ Model for Near-Wall Turbulence and Comparison with Direct Numerical Simulation," NASA TM-103211, 1990.

[6]Lang, N.J., and Shih, T.H., "A Critical Comparison of Two Equation Turbulence Models," NASA TM-105237, 1991.

[7] Yang, Z., and Shih, T.H., "A New Time Scale Based $k-\epsilon$ Model for Near Wall Turbulence," *AIAA Journal*, To appear.

[8]Durbin, P., "Near-Wall Turbulence Closure Modeling with 'Damping Function'," *Theoretical and Computational Fluid Fluid Dynamics*, Vol. 3, 1991, pp 1-13.

[9]Kim, J., Moin, P., and Moser, R., "Turbulent Statistics in Fully Developed Channel Flow at Low Reynolds Number," *Journal of Fluid Mechanics*, Vol. 177, 1987, pp 133-166.

[10]Chien, K.Y., "Predictions of Channel and Boundary Layer Flow with a Low-Reynolds-Number Turbulence Model," *AIAA Journal*, Vol. 20, 1982, pp 33-38.

[11]Spalart, P.R., "Direct Simulation of a Turbulent Boundary Layer up to $Re_\theta = 1410$," *Journal of Fluid Mechanics*, Vol. 187, 1988, pp 61-98.

[12]Wieghardt, K. and Willmann, W., "On the Turbulent Friction Layer for Rising Pressure," NACA TM-1314, 1951.

[13]Herring, H.J., and Norbury, J.F., "Some Experiments on Equilibrium Turbulent Boundary Layers in Favorable Pressure Gradients," *Journal of Fluid Mechanics*, Vol. 27, 1967, pp 541-549.

[14]Samuel, A.E., and Joubert, P.N., "A Boundary Layer Developing in an Increasingly Adverse Pressure Gradient," *Journal of Fluid Mechanics*, Vol. 66, 1974, pp 481-505.

[15]Wilcox, D.C., "Application of Low Reynolds Number Two-Equation Turbulence Models to High Reynolds Number Flows," in *Proc. Near Wall Turbulent Flows*, (ed. R.M.C. So, C.G. Speziale, and B.E. Launder), Elsevier, 1993.

REPORT DOCUMENTATION PAGE

Form Approved
OMB No. 0704-0188

1. AGENCY USE ONLY (*Leave blank*)	2. REPORT DATE	3. REPORT TYPE AND DATES COVERED
	July 1993	Technical Memorandum

4. TITLE AND SUBTITLE

A Galilean and Tensorial Invariant k–ε Model for Near Wall Turbulence

5. FUNDING NUMBERS

WU–505–62–21

6. AUTHOR(S)

Z. Yang and T.H. Shih

7. PERFORMING ORGANIZATION NAME(S) AND ADDRESS(ES)

National Aeronautics and Space Administration
Lewis Research Center
Cleveland, Ohio 44135–3191

8. PERFORMING ORGANIZATION REPORT NUMBER

E–7990

9. SPONSORING/MONITORING AGENCY NAME(S) AND ADDRESS(ES)

National Aeronautics and Space Administration
Washington, D.C. 20546–0001

10. SPONSORING/MONITORING AGENCY REPORT NUMBER

NASA TM–106263
AIAA–93–3105
ICOMP–93–24; CMOTT–93–10

11. SUPPLEMENTARY NOTES

Prepared for the 24th Fluid Dynamics Conference sponsored by the American Institute of Aeronautics and Astronautics, Orlando, Florida, July 6–9, 1993. Z. Yang and T.H. Shih, Institute for Computational Mechanics in Propulsion and Center for Modeling of Turbulence and Transition, NASA Lewis Research Center, (work funded under NASA Cooperative Agreement NCC3-233). ICOMP Program Director, Louis A. Povinelli, (216) 433–5818.

12a. DISTRIBUTION/AVAILABILITY STATEMENT

Unclassified - Unlimited
Subject Category 34

12b. DISTRIBUTION CODE

13. ABSTRACT (*Maximum 200 words*)

A k–ε model is proposed for wall bounded turbulent flows. In this model, the eddy viscosity is characterized by a turbulent velocity scale and a turbulent time scale. The time scale is bounded from below by the Kolmogorov time scale. The dissipation rate equation is reformulated using this time scale and no singularity exists at the wall. A new parameter $R = \frac{k}{Sv}$ is introduced to characterize the damping function in the eddy viscosity. This parameter is determined by local properties of both the mean and the turbulent flow fields and is free from any geometry parameter. The proposed model is then Galilean and tensorial invariant. The model constants used are the same as in the high Reynolds number Standard k–ε Model. Thus, the proposed model will be also suitable for flows far from the wall. Turbulent channel flows and turbulent boundary layer flows with and without pressure gradients are calculated. Comparisons with the data from direct numerical simulations and experiments show that the model predictions are excellent for turbulent channel flows and turbulent boundary layers with favorable pressure gradients, good for turbulent boundary layers with zero pressure gradients, and fair for turbulent boundary layer with adverse pressure gradients.

14. SUBJECT TERMS

Turbulence modeling; k–ε model; Near wall turbulence

15. NUMBER OF PAGES

12

16. PRICE CODE

A03

17. SECURITY CLASSIFICATION OF REPORT	18. SECURITY CLASSIFICATION OF THIS PAGE	19. SECURITY CLASSIFICATION OF ABSTRACT	20. LIMITATION OF ABSTRACT
Unclassified	Unclassified	Unclassified	